

Pseudo-fermionization of 1-D bosons in optical lattices

Guido Pupillo, Ana Maria Rey, Carl J. Williams and Charles W. Clark

National Institute of Standards and Technology, Gaithersburg, MD 20899

(Dated: October 7, 2018)

We present a model that generalizes the Bose-Fermi mapping for strongly correlated 1D bosons in an optical lattice, to cases in which the average number of atoms per site is larger than one. This model gives an accurate account of equilibrium properties of such systems, in parameter regimes relevant to current experiments. The application of this model to non-equilibrium phenomena is explored by a study of the dynamics of an atom cloud subject to a sudden displacement of the confining potential. Good agreement is found with results of recent experiments. The simplicity and intuitive appeal of this model make it attractive as a general tool for understanding bosonic systems in the strongly correlated regime.

Introduction Cold bosonic atoms in optical lattices have recently been used to create quasi-one dimensional systems [1, 2, 3, 4, 5, 6]. In such experiments, arrays of one dimensional tubes are realized by first magnetically trapping a Bose-Einstein condensate (BEC) in a parabolic potential, and then imposing upon it a deep 2D optical lattice, which restricts atomic motions to 1D. These defect-free highly controllable atomic systems offer an excellent opportunity to directly study strongly correlated regimes.

For low densities or large interaction strengths, a 1D gas of ultracold bosons behaves as a gas of impenetrable particles, known as a Tonks-Girardeau (TG) gas. Ref. [7] shows there is a one to one mapping between the eigenenergies and eigenfunctions of TG bosons and the ones of non-interacting fermions, known as fermionization. Two recent experiments [4, 5] successfully reached this parameter regime. In Ref.[5] the TG regime was achieved by adding an optical lattice in the tubes' direction which increases the effective mass and therefore the ratio between interaction and kinetic energy. When the lattice is present and for large enough interactions a commensurate homogenous system not only fermionizes but also undergoes the superfluid to Mott insulator (MI) transition [8]. In the presence of a parabolic trap the MI can be realized for any number of particles [9, 10].

In the TG regime where there is at most one particle per site, single-particle solutions of the periodic plus parabolic potential have been successfully used to describe equilibrium and non-equilibrium properties of the system, both in the presence and in the absence of the MI [9, 10]. However, 1D experiments have been realized in a parameter regime where on-site particle densities are larger than one and standard fermionization is inapplicable [3, 6]. The study of these regimes beyond mean-field has relied mainly on numerical simulations, such as quantum Monte-Carlo or density matrix renormalization group techniques [11, 12, 13, 14]. Here we show that even when the on-site density is larger than one, for a wide range of conditions single-particle solutions can still describe strongly correlated regimes. We call this single-particle approach *pseudo-fermionization* (PF). Comparison with exact Monte-Carlo simulations shows that in the appropriate parameter regimes PF can be used to accurately reproduce equilibrium properties such as the density profile, the momentum distribution, and the ground-state energy.

In the final section we extend our model to treat the non-equilibrium dipole oscillations of atoms subject to a displaced potential, as has been realized in recent experiments [3, 6]. The accuracy and simplicity of the PF method suggest that it is a useful tool for understanding strongly correlated bosonic systems.

Bose-Hubbard Hamiltonian The Bose-Hubbard (BH) Hamiltonian describes the system's dynamics when the lattice is loaded such that only the lowest vibrational level of each lattice site is occupied and tunneling occurs only between nearest-neighbors [15]

$$H = -J \sum_{\langle i,j \rangle} \hat{a}_i^\dagger \hat{a}_j + \frac{U}{2} \sum_j \hat{n}_j (\hat{n}_j - 1) + \Omega \sum_j j^2 \hat{n}_j. \quad (1)$$

Here \hat{a}_j is the bosonic annihilation operator of a particle at site j , $\hat{n}_j = \hat{a}_j^\dagger \hat{a}_j$, and the sum $\langle i, j \rangle$ is over nearest neighbors. In Eq.(1) the hopping parameter J , and the on-site interaction energy U are functions of the lattice depth V_o . Ω is proportional to the curvature of the parabolic potential.

Homogeneous system For a homogeneous system ($\Omega = 0$) with N atoms and M sites the spectrum is fully characterized by the ratio between interaction and hopping energies $\gamma = U/J$, and by the filling factor $N/M = (n-1) + \Delta N/M$. Here n is the smallest integer larger than N/M and $\Delta N < M$. If the lattice is commensurately filled ($\Delta N = 0$) and $\gamma > \gamma_c(n-1)$, the ground state is a Mott insulator with reduced number fluctuations. The critical value γ_c is about 4 according to numerical results [16]. For the incommensurate case, *i.e.* $\Delta N > 0$, the ground state is a superfluid. In this case, if $\gamma/n \gg \gamma_c$ the extra atoms can be thought of as TG bosons with effective hopping energy nJ on top of a Mott state with filling factor $n-1$. This is justified because the population of states with more than n atoms per site is suppressed by a factor of the order of J/U . The lowest $M!/((\Delta N)!(M-\Delta N)!)$ eigenstates and eigenenergies can then be described by means of the standard Bose-Fermi mapping with J replaced by nJ . We refer to this approach as *pseudo-fermionization*.

Inhomogeneous system When the parabolic trap is present ($\Omega > 0$), the density profile of the atomic cloud is determined by an interplay of U , J , Ω and N . The system is fermionized

if [9]

$$\gamma > \gamma_c, \quad U > \Omega((N-1)/2)^2. \quad (2)$$

While the first inequality is the same as for homogeneous lattices, the second one is specific for trapped systems and is necessary to suppress multiple occupancy of single sites. In this fermionized regime, for decreasing J the density at the trap center increases, and, when the condition $2J \lesssim \Omega((N-1)/2)^2$ is satisfied, sites around the trap center begin to have unit filling [9, 10]. If the inequality

$$J < \Omega N, \quad (3)$$

is also satisfied, the ground state is a unit-filled Mott state in all N sites. In this case, fluctuations occur mainly at the edge of the density distribution, due to tunneling of atoms to empty sites. Such fluctuations are proportional to ΩN , which is the trap gradient at the site $(N-1)/2$. Residual fluctuations at the trap center are due to mixing of particle-hole excitations and are proportional to $2\sqrt{2}(J/U)$.

For $\Omega((N-1)/2)^2 \gtrsim U$ it is energetically favorable for atoms to pile up at the trap center. In fact, superfluid and Mott insulator phases with different filling factors can coexist, due to the interplay between on-site interactions and the external potential [11, 15, 17]. In the trivial case $J = 0$, Fock states with a definite number of atoms in each site are eigenstates of the Hamiltonian. The density profile results into a “cake”-like structure with maximal occupation n_{max} at the trap center if

$$2H_{n_{max}-1}^{(1/2)} < \left[(N - n_{max})\sqrt{\Omega/U} \right] < 2H_{n_{max}}^{(1/2)}, \quad (4)$$

where $H_n^{(1/2)} \equiv \sum_{i=0}^n \sqrt{i}$ [17]. The number of atoms N_n in the n^{th} “cake” layer is given by $(N_1 - N_n)(N_1 + N_n - 2) = 4U(n-1)/\Omega$ with the normalization condition $\sum_{n=1}^{n_{max}} N_n = N$. Similar to the PF in the homogeneous case, we can view the atoms in each layer as creating an independent Mott state with unit filling. For finite but small values of J , all layers except the top one can still be thought of as an independent Mott state with filling factor one if

$$\gamma > \gamma_c(n_{max} - 1), \quad \Omega N_{n_{max}-1} > J(n_{max} - 1). \quad (5)$$

In analogy to Eq. (2) the first inequality insures that in each layer with $n < n_{max}$ the average kinetic energy required for one atom to hop from one site to the next is insufficient to overcome the potential energy cost and therefore particle-hole excitations are suppressed by a factor of order nJ/U . The second inequality guarantees that in all but the n_{max}^{th} layer number fluctuations are confined mainly at the edge of the Mott state, in analogy to Eq.(3).

Under a wide range of relevant experimental parameter regimes the above conditions are satisfied and fluctuations in the various layers do not spatially overlap. If also

$$\gamma > \gamma_{n_{max}}, \quad (6)$$

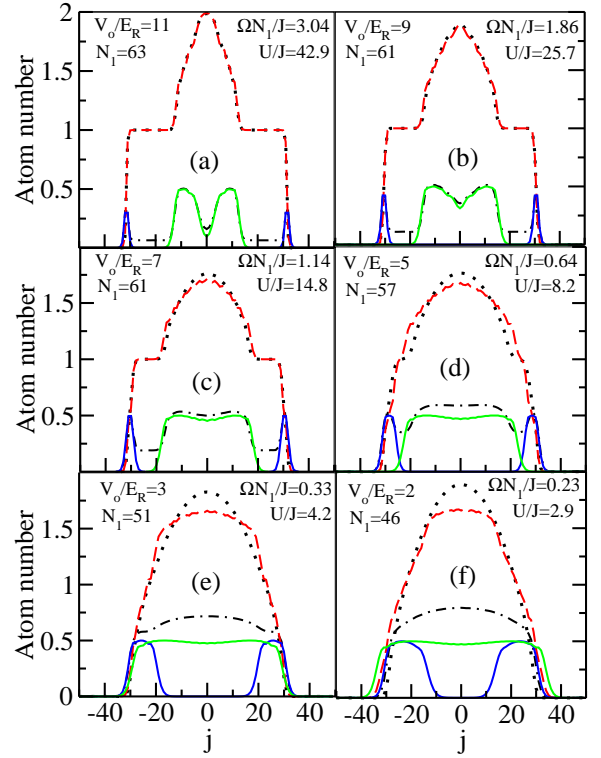


FIG. 1: Local densities $\langle \hat{\rho}_j \rangle$ and fluctuations $\langle \Delta \hat{\rho}_j^{(n)} \rangle$ as a function of the site index j . Dotted(black) and dashed(red) lines are the numerical and analytical densities, respectively. The dashed-dotted(black) line is the numerical fluctuation, while solid-black(blue) and solid-grey(green) lines are the analytical fluctuations for the lower($n = 1$) and upper($n = 2$) layers, respectively.

to a very good approximation atoms in all layers can be treated as TG bosons with an effective hopping energy nJ . Notice that atoms in the top layer do not need to be localized. Under these conditions, single-particle solutions can be successfully used to obtain expressions for all many-body observables. This is the generalization of PF to trapped systems.

In the following we show the success and the limitations of this approach, by applying it to a system with the same parameters as the ones used in an experiment recently performed at NIST [6].

Numerical comparisons In the NIST experiment [6] approximately $N_T = 1.4 \times 10^5$ ^{87}Rb atoms were trapped in an array of one-dimensional tubes with $N \simeq 80$ atoms in the central tube. An additional periodic potential was added along the direction of the tubes and its depth V_o was varied for different experiments. The frequency of the parabolic potential in the tubes’ direction was such that $\Omega = 7.4 \times 10^{-4} E_R$, with E_R the photon recoil energy. Here we focus on the central tube only and consider $V_o > 2E_R$, where the tight-binding Hamiltonian Eq.(1) is expected to be valid. For these parameters, Eq. (4) yields $n_{max} = 2$.

In Fig. 1 we show comparisons between the density and number fluctuations for the central tube calculated by using

the PF approximation and exact quantum Monte-Carlo numerical simulations based on the Worm algorithm [18], for lattice depths $V_o/E_R = 11(a), 9(b), 7(c), 5(d), 3(e), 2(f)$. In the numerical simulations the temperature is $0.01J$. In the plots the dotted(black) and dash-dotted(black) lines correspond to the density and number fluctuations as numerically calculated by using the Monte-Carlo code, respectively. The dashed(red), the solid-black(blue) and solid-grey(green) lines correspond to the density $\langle \hat{\rho}_j \rangle$, and to the number fluctuations for the atoms in the first $\langle \Delta \hat{\rho}_j^{(1)} \rangle$ and second layer $\langle \Delta \hat{\rho}_j^{(2)} \rangle$, as calculated with the PF model respectively. In particular, the density is given by $\langle \hat{\rho}_j \rangle = \sum_{s=0}^{N_1-1} |f_j^{1(s)}|^2 + \sum_{s=0}^{N_2-1} |f_j^{2(s)}|^2$ where $\{f_j^{n=1,2(s)}\}$ are the s^{th} single-particle eigenmodes of Eq.(1) with hopping energies nJ respectively and j is the lattice site index. The fluctuations are given by $\langle \Delta \hat{\rho}_j^{(n)} \rangle = \sqrt{\sum_{s=0}^{N_n-1} |f_j^{n(s)}|^2 - \left(\sum_{s=0}^{N_n-1} |f_j^{n(s)}|^2\right)^2}$.

The conditions for PF to be applicable, Eqs.(5) and (6), are strictly valid for $V_o \gtrsim 5E_R$. Consistently, Fig. 1(a-c) shows that for $V_o/E_R = 11, 9, 7$ the density profile and number fluctuations are very well reproduced by the model, except for the finite value of the fluctuations in the flat region of the density profile. These small fluctuations of order $2\sqrt{2}J/U$ are due to the particle-hole excitations which are neglected in the model. The model predicts that some sites at the trap center have exactly a filling factor of two when $2(2J) \lesssim \Omega((N_2 - 1)/2)^2$. This condition is fulfilled for $V_o = 11E_R$, and in fact a flat density distribution with two atoms per site is observed in Fig.1-(a) at the trap center, both in the analytical and numerical results. This confirms the validity of the idea of thinking of the atoms in the second layer as TG-bosons with effective hopping energy $2J$.

For $V_o = 5E_R$, γ is barely $2\gamma_c$, and $\Omega N_1 < J$ so that fluctuations at the edge of the first layer extend far enough to overlap with the ones of the second layer. We only expect PF to give qualitative predictions in this regime. For $V_o = 3, 2E_R$ the conditions Eqs.(5) and (6) are not satisfied, and the model fails to reproduce the exact results. Nevertheless, we notice that the PF model predicts the formation of a Mott state in the lowest layer for $V_o \gtrsim 3E_R$ because $\gamma \approx \gamma_c$ and $\Omega(N_1 - 1)^2/4 > 2J$ at $3E_R$. The numerically obtained fluctuations show the appearance of a flat region at the cloud's edge for $V_o = 3E_R$. Such flat region signals the formation of a Mott state as it evolves for deeper lattices into the observed dip in the fluctuations and disappears for shallower lattices (Fig 1-(e)).

In Fig.2 we compare the momentum distribution $\rho(k)$ for the many-body system, solid(black) line, with the one predicted by the PF model, dashed(red) line, for $V_o = 11(a), 9(b), 7(c)$, and $5(d)$. The model curves are given by $\rho(k) = \rho(k)^{(1)} + 2\rho(k)^{(2)} - N_2/M$, where $\rho(k)^{(n=1,2)}$ are the momentum distributions for N_n TG bosons with effective hopping rate nJ , calculated numerically with the Monte-Carlo code. For all curves, the height of the central peak is larger and the width at half maximum is smaller for the exact than for the model solutions. This is expected because

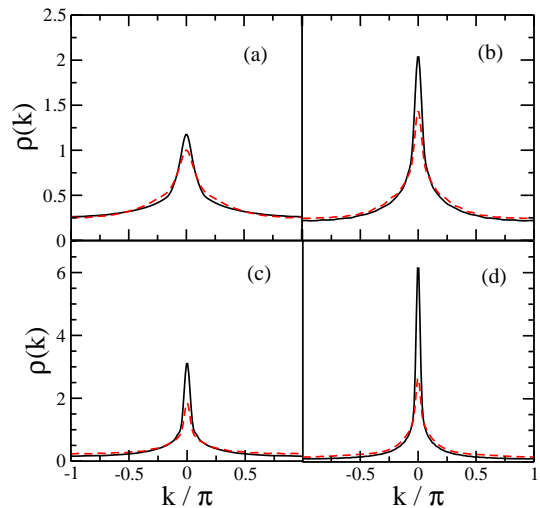


FIG. 2: Momentum profiles $\rho(k)$ as a function of the momentum k , for lattice depths $V_o/E_R = 11(a), 9(b), 7(c)$, and $5(d)$. The solid(black) and dashed(red) lines are the exact momentum distributions and the model momentum distributions, respectively.

the model neglects correlations between atoms in the first and second layers. However, the agreement is at least qualitative for all displayed lattice depths where PF applies. On the other hand the agreement for the deepest lattice in consideration is worse than the one found for the local observables $\langle \hat{\rho}_j \rangle$ and $\langle \Delta \hat{\rho}_j \rangle$, (Fig 1). This is consistent with previous observations for standard fermionization [19].

In Fig. 3 ground state energies are compared as a function of lattice depth. The solid(black) line is calculated numerically using the Monte-Carlo algorithm and the dashed(red) line using the PF model $E = \sum_{s=0}^{N_1-1} E_1^{(s)} + \sum_{s=0}^{N_2-1} (U + E_2^{(s)})$. Here, $E_{1,2}^{(s)}$ are the s^{th} single-particle eigenenergies of systems with hopping energies J and $2J$, respectively. At $V_o = 5E_R$ the model predicts a ground-state energy which is 10% larger than the numerical solution while at $V_o = 11E_R$

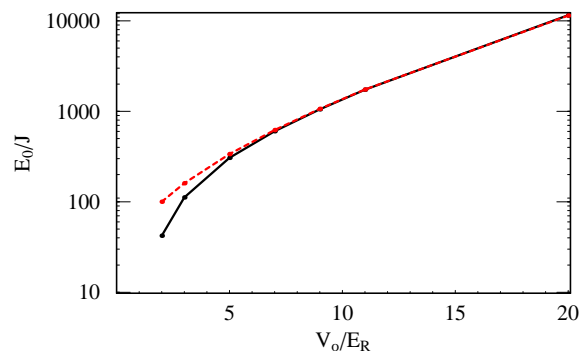


FIG. 3: Energy as function of V_o/E_R . The solid(black) and dashed(red) lines are the numerical and analytical energies, respectively.

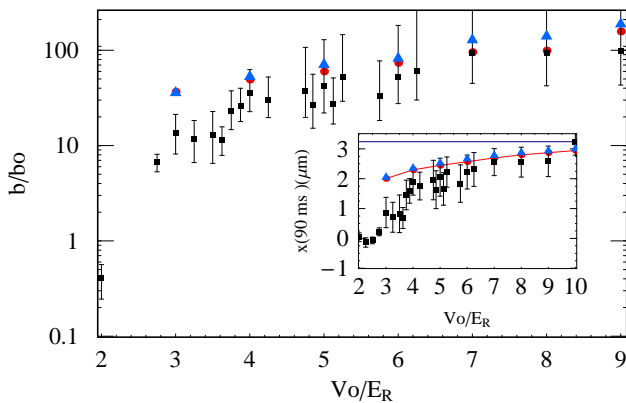


FIG. 4: Damping rate of dipole oscillations b as a function of V_o/E_R . b is in units of $b_o = 2m\omega_T$. The squares are the NIST experimental results. The circles (red) are the model results for the central tube, and the triangles (blue) are the model results averaged over all the tubes. Inset: center of mass position after 90 ms.

the difference decreases to only 0.4%. This also confirms the validity of the PF model as the lattice deepens.

Center of mass oscillations In the NIST experiment [6], center of mass oscillations were induced by a sudden displacement of the harmonic potential by $\delta = 8$ lattice sites. An overdamped motion was observed for lattice depths $V_o \gtrsim 3E_R$. The damping rate b was obtained by fitting to the formula $m^*\ddot{x} = -b\dot{x} - m\omega_T^2x$, where m and m^* are the atomic and effective masses and ω_T is the magnetic trapping frequency. Previous theoretical analysis of the damping did not use real experimental parameters [9, 20, 21, 22] or were not applicable in the strongly correlated regime [23, 24]. Here we show that the PF approach reproduces well the experimental results in the overdamped regime. In Fig.4 the experimental data (black squares) are compared to the predictions of the PF model. In the model, the center of mass position of the atoms in the central tube (red dots) is given by $x(N) = a/N \left[\sum_{s=0}^{N_1-1} x_1^{(s)}(t, N) + \sum_{s=0}^{N_2-1} x_2^{(s)}(t, N) \right]$, where

$$x_n^{(s)}(t, N) = \sum_{k,l,j} j c_l^{n(s)} c_k^{n(s)} e^{-i(E_n^{(k)} - E_n^{(l)})t/\hbar} f_j^{n(k)} f_j^{n(l)}. \quad (7)$$

Here, N is the number of atoms in the central tube, a is the lattice spacing and the coefficients $c_k^{n(s)} = \sum_j f_j^{n(k)} f_{j-\delta}^{n(s)}$ are the projection of the s^{th} excited state of the displaced potential onto the k^{th} excited eigenstate of the undisplaced potential for atoms in the $n = 1, 2$ layer, respectively. The PF model is expected to give an accurate description of the center of mass oscillations if during the dynamics the atoms in the first and second layer can still be treated as independent objects, *i.e.* when number fluctuations in the two layers do not overlap during the evolution. Because in the experiment the measured damping rate was an average over all

the tubes, in Fig.4 we also plot the model's prediction for the average damping rate (blue triangles). The latter was calculated assuming that all tubes evolve independently and therefore that $x(t) = \left[\sum_{\mathcal{N}=1}^N \mathcal{N} P(\mathcal{N}) x(\mathcal{N}, t) \right] / \sum_{\mathcal{N}=1}^N P(\mathcal{N}) \mathcal{N}$ is the average center of mass position. Here, $P(\mathcal{N})$ is the probability of having a tube with \mathcal{N} atoms. Assuming an initial Thomas-Fermi distribution of the 3D system, $P(\mathcal{N}) \approx 2/3(N^2\mathcal{N})^{-(1/3)}$ [5].

When there is at most one atom per site, atoms in the Mott state have been shown to be responsible for the overdamped dynamics [9, 22]. Here, the two-layer model predicts that a Mott state is created in the lowest layer for $V_o \gtrsim 3E_R$, Fig.1, and therefore atoms in this layer are almost frozen. However, atoms in the second layer are not necessarily localized, and their dynamics can be underdamped. Because there are always more atoms in the lowest layer than in the upper one, the overall dynamics is overdamped, and this explains the large damping observed in the experiment for $V_o \gtrsim 3E_R$. This is also in agreement with the qualitative explanation of the damping given in Ref.[3].

Strictly speaking, the fluctuations in the two layers do not overlap during the dynamics only for $V_o > 7E_R$, thus we expect the model to be valid for the deepest lattice depths only. Nevertheless, Fig.4 shows that the theoretical calculations are within the experimental error bars already for $V_o \gtrsim 4$. Figure 4 also shows that the damping rates for the central tube and the average are very similar, and this is because tubes with about $N = 80$ atoms have the largest weight. The average shows a larger damping because it takes into account contributions from tubes that do not have extra atoms in the second layer. In the inset we also compare the experimental center of mass position of the atomic cloud after 90ms with the model solutions. The agreement between experiment and theory is consistent with the one found for the damping rate.

Summary We have developed a simple model that generalizes the Bose-Fermi mapping to regimes where the filling factor is larger than one. The model is relevant for 1D trapped gases where the co-existence of Mott-insulating regions with different occupation numbers is permitted. We presented the necessary conditions for the model to be valid and showed the usefulness and limitations of the method by comparing its predictions for some physical observables with numerical Monte-Carlo simulations. Very good agreement between the model and the numerical solutions was found in the parameter regime where the model is valid. Finally we used the PF model to study the overdamped dynamics of the center of mass after a sudden displacement of the trapping potential, and found good agreement with recent experiments. In particular, the overdamped motion was linked to the presence of a Mott state in the lowest atomic layer.

The authors thank Trey Porto and Jamie Williams for discussions, and Nikolay V. Prokof'ev for discussions and for providing the Monte-Carlo code. This research was supported in part by ARDA/NSA.

-
- [1] B. Laburthe Tolra *et al.*, Phys. Rev. Lett. **92**, 190401 (2004).
[2] H. Moritz *et al.*, Phys. Rev. Lett. **91**, 250402 (2003).
[3] T. Stöferle *et al.*, Phys. Rev. Lett. **92**, 130403 (2004).
[4] T. Kinoshita *et al.*, Science **305**, 1125 (2004).
[5] B. Paredes *et al.*, Nature **429**, 277 (2004).
[6] C. D. Fertig *et al.*, Phys. Rev. Lett. **94**, 120403 (2005).
[7] M. Girardeau, J. Math. Phys. **1**, 516 (1960).
[8] M. P. A. Fisher *et al.*, Phys. Rev. B **40**, 546 (1989).
[9] A.M. Rey *et al.*, cond-mat/0503477 (2005).
[10] M. Rigol and A. Muramatsu, Phys. Rev. A **70**, 043627 (2004).
[11] G. G. Batrouni *et al.*, Phys. Rev. Lett. **89**, 117203 (2002).
[12] V. A. Kashurnikov *et al.* Phys. Rev. A **66**, 031601 (2002).
[13] C. Kollath *et al.*, Phys. Rev. A **69** 031601 (2004).
[14] A. J. Daley *et al.*, J. Stat. Mech.: Theor. Exp. **P04005** (2004).
[15] D. Jaksch *et al.*, Phys. Rev. Lett. **81**, 3108 (1998).
[16] J. K. Freericks and H. Monien, Phys. Rev. B **53**, 2691 (1996).
[17] B. DeMarco *et al.*, cond-mat/0501718 (2005).
[18] N. V. Prokof'ev *et al.*, Phys. Lett. A **238**, 253 (1998); JETP **87**, 310 (1998).
[19] L. Pollet *et al.*, Phys. Rev. Lett. **93**, 210401 (2004).
[20] A. Polkovnikov and D.-W. Wang, Phys. Rev. Lett. **93**, 070401 (2004).
[21] E. Altman *et al.*, cond-mat/0411047 (2004).
[22] M. Rigol *et al.*, cond-mat/0503302 (2005).
[23] J. Gea-Banacloche *et al.*, cond-mat/0410677 (2004).
[24] J. Ruostekoski and L. Isella, cond-mat/0504026 (2005).